Energy & Environmental Science

PAPER

View Article Online
View Journal | View Issue

Cite this: *Energy Environ. Sci.*, 2018, **11**, 1536

A comparative technoeconomic analysis of pathways for commercial electrochemical CO_2 reduction to liquid products†

Joshua M. Spurgeon *[a] and Bijandra Kumar[b]

Received 10th January 2018,
Accepted 29th March 2018

DOI: 10.1039/c8ee00097b

rsc.li/ees

Electrochemical reduction of CO_2 to fuels and chemicals is currently a focus of significant research effort as a technology that can simultaneously mitigate greenhouse gas emissions while storing renewable electricity for use on demand. Liquid products are particularly desirable as an easily storable and portable energy-dense form. To be widely implemented, CO_2 electroreduction technologies must be able to produce chemicals at costs that are economically competitive with existing commercial prices. In this work, four possible routes to the electrochemical synthesis of liquid products from CO_2 derived from post-combustion flue gas were compared with one consistent approach to technoeconomic analysis. In the first case, diesel fuel was produced from electrosynthesized CO plus H_2 to make syngas which was subsequently converted through the Fischer–Tropsch process. Liquid ethanol was modeled through two comparable approaches, a one-step electrolysis and a two-step cascade electrolysis. Lastly, the direct electrosynthesis of formic acid from CO_2 was considered. In the base case scenarios established on current state-of-the-art CO_2 reduction research, none of the processes were modeled to be competitive with present fuel prices. High capital expense for the electrolyzer units was the primary limiting factor. With conceivable improvements in an optimistic scenario, the diesel process was projected to have the best pathway to making cost-effective fuels, while ethanol would be prohibitively expensive without major improvements to the present electrosynthesis performance. Formic acid, though projected to be expensive relative to its stored energy content, was projected to have perhaps the simplest pathway to production at costs competitive with its commercial bulk price. In each case, the levelized cost of the liquid product was most strongly influenced by parameters that affect the electrolyzer capital cost (*i.e.*, current density, faradaic efficiency, and cost per electrode area).

Broader context

Carbon dioxide emissions are a source of increasing concern across the world, with many researchers pushing for advances in carbon capture, sequestration, and utilization to be developed in conjunction with renewable energy technology. Researchers and industries have shown a growing interest in utilizing waste CO_2 to generate profitable products while simultaneously reducing greenhouse gas emissions. One common goal is to pursue electrochemical CO_2 reduction to fuels as a route for the energy storage of intermittent renewable electricity such as wind and solar. In particular, hydrocarbon and oxygenate liquid products such as gasoline, diesel, ethanol, *etc.*, are quite energy-dense by volume relative to hydrogen or batteries and are thus an ideal fuel for applications such as transportation. However, for any chance at commercialization, liquid products synthesized *via* electrochemical CO_2 reduction must be economically competitive with the market prices for equivalent fuels produced through traditional methods. Technoeconomic analyses are a useful tool to provide researchers with insight on how different approaches compare in terms of the overall process costs that could be expected at the industrial scale. Such analyses can also highlight the relative importance of key technological performance parameters on the final cost of product and help to guide research priorities.

Introduction

The rising concentration of CO_2 in the atmosphere has been a cause for global concern because the greenhouse gas properties of CO_2 are believed to contribute to climate change. While it is thus imperative to deal with carbon emissions for environmental reasons, increasingly there has been interest in utilizing

---

[a] *Conn Center for Renewable Energy Research, University of Louisville, Louisville, Kentucky, 40292, USA. E-mail: joshua.spurgeon@louisville.edu*

[b] *Department of Technology, Elizabeth City State University, Elizabeth City, NC 27909, USA*

† Electronic supplementary information (ESI) available. See DOI: 10.1039/c8ee00097b

waste CO_2 for economically beneficial processes. There are potential commercial applications for CO_2 in refrigeration, fire extinguishers, the beverage industry, and hydraulic fracturing (*i.e.*, fracking) for fossil fuels.[1] However, by converting CO_2 to useful fuels and chemicals, numerous commercial pathways become a possibility.[2] This conversion of CO_2 can require significant energy input and thus is only logical if the energy comes from carbon-emission-free sources such as renewable solar and wind energy. In fact, using intermittent renewable electricity to convert CO_2 can serve as an energy-dense storage mechanism for these sources, providing greater reliability and permitting their use in intensive portable applications such as transportation. Liquid carbonaceous fuels have significantly higher volumetric energy density than batteries and even compressed hydrogen.[3]

Renewable electricity can drive the conversion of CO_2 to fuels and chemicals through the electrochemical carbon dioxide reduction reaction (CO2RR).[4–7] Extensive work has been devoted to the development of heterogeneous electrocatalysts with high selectivity and low overpotential for CO2RR. Electrocatalysts for CO2RR have thus far generally fallen into one of four types, depending on the surface binding energy to the CO_2 reduction reaction intermediates, which affects the rate-limiting step and promotes a specific mechanistic pathway.[8,9] Surfaces which are favorable for hydrogen evolution, such as Pt, make poor catalysts for CO_2 conversion because CO2RR is unable to compete kinetically with the formation of H_2 in aqueous media. Many metals, including Ag and Au, selectively promote the formation of CO at high selectivity.[10–14] A few other catalysts, including Sn and Pb, promote a different branching of the reaction pathway upon adsorption of CO_2 and lead to high selectivity for formic acid/formate ($HCOOH/HCOO^-$).[15–21] Only a few electrocatalyst materials, most notably Cu, produce other hydrocarbon species in appreciable yield by further reduction to methane, ethylene, ethanol, and small amounts of other products.[22–27] An economically viable pathway to commercial electrochemical CO_2 conversion will thus likely have to rely on a high-selectivity electrosynthesis of one of these favored products.

Some previous efforts to analyze the technoeconomic feasibility of specific CO_2 electroreduction processes have been reported.[15,28–30] Herein we employ one consistent method of technoeconomic analysis to compare four possible routes which use electrochemical CO_2 reduction to produce a liquid product, as outlined in Fig. 1. A liquid product, particularly an energy-dense fuel, would be a very desirable outcome for CO_2 conversion that could be easily stored and transported, and used on-demand for energy-intensive applications. While other liquids are conceivable, the catalyst selectivity limitations outlined above have led us to model the processes for the synthesis of three promising end products: diesel fuel, ethanol, and formic acid. Diesel fuel, though not produced directly through CO2RR, can be made in high yield through the Fischer–Tropsch conversion of syngas, a mixture of CO and H_2.[28,31–33] Therefore, in the first case for analysis, the electrosynthesis of CO provides the feedstock to a syngas mixture for the Fischer–Tropsch synthesis of liquid fuel (FTL). This is designated the CO_2–CO–FTL process. High faradaic efficiency (FE) CO_2 electroreduction to CO at low overpotential has already been demonstrated,[14] and a few start-up companies are working to commercialize this technology.[34] The next case considered is the direct electroreduction of CO_2 to ethanol (CO_2–C_2H_5OH). Controlling the reaction to provide high selectivity for this two-carbon product is much more challenging, and it involves a non-electrochemical step for the adsorption of single-carbon species to adjacent sites to enable C–C bond formation. Several efforts to develop electrocatalysts for a direct conversion of CO_2 to C_2H_5OH have shown marginal faradaic efficiencies but generally required high overpotentials.[25–27,35–38] The third route to a liquid product also targets ethanol but uses a two-step cascade electrochemical synthesis approach to synthesize C_2H_5OH at a higher total yield. CO_2 is first converted to CO with high selectivity[14] and subsequently the CO is electroreduced to C_2H_5OH at low overpotential with fairly high selectivity.[39,40] The two-step CO_2 to ethanol cascade (CO_2–CO–C_2H_5OH) breaks the complicated 12-electron ethanol synthesis into two separate reactions, and each individual reaction can be operated with the optimal choice of catalyst, temperature, applied bias, *etc.*, to maximize yield and minimize overpotential. Lastly, a route for the direct electrochemical conversion of CO_2 to formic acid is considered (CO_2–HCOOH). Like CO electrosynthesis, the formation of HCOOH has been demonstrated with high faradaic efficiency with impressive stability, though it has required notably greater applied potential.[41] Established technoeconomic analysis methodology was employed to explore the economic feasibility of these possible routes to commercial electrochemical reduction of CO_2 to liquid products.

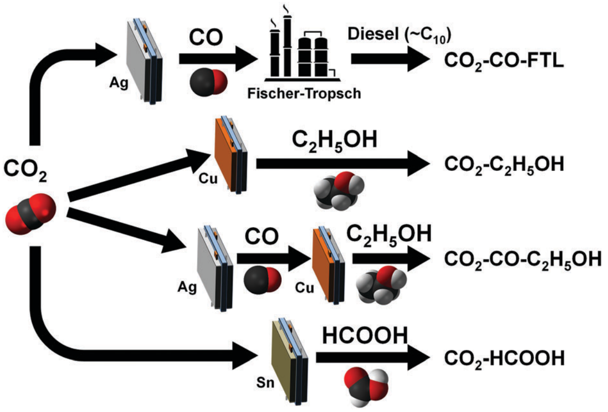

Fig. 1 Schematic of the four chosen pathways for electrochemical CO_2 reduction to liquid products for technoeconomic analysis. The pathways are CO_2 electroreduction to (1) CO and subsequent Fischer–Tropsch conversion of syngas to diesel fuel (CO_2–CO–FTL), (2) ethanol in one step (CO_2–C_2H_5OH), (3) CO and subsequent reduction to ethanol in two steps (CO_2–CO–C_2H_5OH), and (4) formic acid (CO_2–HCOOH).

Methodology

Capital cost analysis

All four scenarios for an electrochemical CO_2 reduction plant used the base-case design specifications and financial parameters listed in Table 1. Each facility was sized to handle the emissions from a 500 MW coal-powered electric utility as

Table 1 Operating and financial parameters used for each system

Parameter	Value
Basis power utility size	500 MW
CO_2 conversion plant lifetime	20 years
$ basis year	2018
Inflation rate	1.9%
Discount rate (r)	12%

described under the Technoeconomic assumptions. The facility and capital equipment were assumed operational over a 20 year lifetime in each case. All capital costs and results were adjusted from the relevant source material to account for inflation and modified to 2018 dollar estimates.

Net present value analysis

For each CO_2 reduction process and each sensitivity case evaluated, a standard discounted cash flow analysis was used over the assumed 20 year plant lifetime to determine a levelized cost of fuel (LCF) for each liquid product. The capital expense of each plant was assumed to be incurred during a one-year construction period (*i.e.*, year 0), while the operating expenses and product revenue were generated each year for 20 years and were discounted to the year of construction using a standard discount rate, r, of 12% according to the equations below:[42]

$$\text{Operating cost PV} = \sum_{i=1:n}^{n} \frac{\text{OC}_i}{(1+r)^i} \qquad (1)$$

$$\text{Product revenue PV} = \sum_{i=1:n}^{n} \frac{\text{PR}_i(\text{LCF})}{(1+r)^i} \qquad (2)$$

$$\text{NPV} = 0 = \text{Product revenue PV (LCF)} - \text{Operating cost PV} - \text{capital expense} \qquad (3)$$

where PV is the present value, OC is the operating cost and PR is the product revenue (a function of the LCF) at each year i, and NPV is the net present value. Replacement costs for electrolyzer parts were included as operating expenses every seven years. Calculations did not apply depreciation to capital assets and assumed a pre-tax environment. The LCF for the respective liquid product in each analyzed CO_2 reduction pathway was determined by adjusting its value to result in a final net present value (*i.e.*, the sum of the capital expense and the discounted present value of the operating costs and product revenue) equal to zero.

Technoeconomic assumptions

Power plant

In each case, the source of the CO_2 feedstock is assumed to be from the post-combustion output flue gas from a pulverized-coal-fired power plant. The basis for technoeconomic analysis in all four scenarios is a 500 MW power plant.[28] The average CO_2 emission rate without carbon capture technology for a number of mostly bituminous coal power plants was taken as 820 kg MWh^{-1}.[43] The capital and operating costs of the power plant are not directly included in the economics of the CO_2 conversion analysis, but these costs are incorporated through the price of electricity purchased from the grid.

CO_2 capture

To extract concentrated CO_2 from the power plant post-combustion exhaust, a proven carbon capture technology is required. Amine-based solvents are often used for CO_2 capture from flue gas, with monoethanolamine (MEA) a commonly employed solvent. In a packed absorption column, the MEA reacts with and absorbs CO_2 to form an MEA carbamate soluble salt. This CO_2-rich MEA solution is then sent to a heat exchanger at ~120 °C and fed to a stripping column where the MEA is regenerated and recycled while the concentrated CO_2 stream is released for further processing.[44] The key parameters for CO_2 capture from a coal-fired power plant using MEA are contained in Table S1 (ESI†).[43] The average CO_2 emission rate for coal plants with capture technology was 111 kg MWh^{-1}, with an average CO_2 capture rate of 709 kg MWh^{-1} available for downstream conversion by electrochemical reduction. Capital and operating costs for the CO_2 capture process were included in the technoeconomic analysis. Because the capture process is upstream of the electrochemical CO_2 reactor, these costs were identical for all four scenarios. The power plant overnight capital costs for carbon capture were taken at an inflation-adjusted average of \$1878 kW^{-1}, where overnight costs include pre-construction, contingency, engineering, procurement, and construction costs.[43] In addition, the carbon capture process is reported to cause an estimated decrease of 25% in the net efficiency of power generation. This loss was accounted for in the operating costs of the capture process as an annual electricity demand (Table S1, ESI†).

CO_2 electrolyzers

The critical component in the electrochemical CO_2 reduction process is the CO_2 electrolyzer. This unit must integrate the fundamental research on CO2RR electrocatalysis into a scaled-up reactor which incorporates state-of-the-art anode catalysts for water oxidation, an appropriate membrane for product separation and preventing species crossover, and well-designed electrodes for effective mass-transport and high current density. The critical operating metrics for the electrolyzer are the cell voltage, the current density, and the faradaic efficiency for the desired product. The electrolyzer cell voltage, V, is the two-electrode bias applied between the anode and cathode at the operating condition, which includes the thermodynamic potential required for the relevant CO_2 reduction reaction as well as activation overpotentials at the anode and cathode plus ohmic overpotential associated with resistances in the electrodes and membrane. A high current density, J, in the electrolyzer, which requires fast mass transport of the reactants to the electrocatalyst surface, is desirable to minimize the total capital expense of the electrolysis system to achieve a given product formation rate. Likewise, the faradaic efficiency, ε, which is the percentage of charge passed in the electrolyzer that was directed towards the formation of a specific product, should be as close to 100% as possible for the desired liquid product in order to minimize capital expense as well as energy loss to byproducts. The required electricity consumption, E, in a given period of time, t, for the electrolyzer system was calculated by:

$$E = \frac{n_i F X_i V t}{\varepsilon_i} \quad (4)$$

where n is the number of electrons per molecule of the product i, F is Faraday's constant, and X is the molar production rate of the product.

Electrochemical CO_2 reduction is in many ways analogous to water electrolysis, and thus commercial CO_2 electrolyzers are expected to share many design features with water electrolyzers. Although the membrane material and cathode electrocatalyst are distinct, commercial CO_2 electrolyzers are thus far quite similar to proton exchange membrane (PEM) water electrolyzers with the same general architecture and required components.[34,41] Established sophisticated models for the costs of PEM electrolysis technology to produce H_2 from water were therefore utilized to estimate the capital expense for CO_2 electrolyzers. In particular, the US Department of Energy Hydrogen Analysis (H2A) project has published case studies for the technoeconomic analysis of hydrogen production, and the case for central grid PEM electrolysis was leveraged for this study.[45] As listed in Table S2 (ESI†), the reference parameters for the PEM electrolysis were used to calculate a capital cost per area of the electrodes. Including both stack costs and balance of plant (BOP) costs, the inflation-adjusted uninstalled electrolyzer cost was \$30 927 m^{-2}. Capital expenses for a full plant must include additional indirect costs as well, including installation (12% of the uninstalled cost), contingency (15% of installed capital cost), site preparation (2% of installed capital cost), engineering and design (8% of installed capital cost), and up-front permitting (15% of installed capital cost).[42,45,46] These capital costs per area do not account for electrolyzer down time for maintenance, and thus an electrolyzer capacity factor of 97% was assumed when determining the total electrode area required to meet the annual production rate.[45,46] For the four CO_2 reduction processes analyzed, the total electrode area required was determined from the liquid product formation rate, the electrolyzer current density, and the respective faradaic efficiency. This cost model per electrode area was assumed valid for the base case capital expense associated with each type of CO_2 or CO electrolyzer throughout the study.

Furthermore, electrolyzer components can break down or wear out over time, necessitating repairs over the course of the plant lifetime. Costs for replacement of the major components every seven years (*i.e.*, at years 7 and 14) were calculated at 15% of the electrolyzer installed capital expense.[42,45,46] Thus, the base case scenario for each process in this study assumes stability of the electrolyzer components and CO2RR electrocatalyst commensurate with this replacement rate. All other system capital was assumed to remain functional over the lifetime of the plant. The base case single-pass conversion of CO_2 within the electrolyzer was assumed to be 50%, which would vary somewhat depending on reactor design.[28] With the preceding assumptions, the resulting capital expense per electrode area for the CO_2 electrolyzer was significantly higher than reported in a previous study.[28] The numbers used herein reflect the full capital costs for a PEM electrolyzer plant based on the most current H2A model.[45] However, the base case cost per electrode area assumes a linear scaling, and a more aggressive scaling factor will result in a reduced capital expense. For the present study, reduced cost due to scaling is limited to the sensitivity analysis and the parameters for the optimistic case.

Gas separation

Because of incomplete conversion of the CO_2 reactant passing through the electrolysis system, it is beneficial to separate unreacted CO_2 from the other gaseous products and recycle it back to the process upstream of the electrolyzer. This ensures much greater conversion of CO_2 and lowers the cost of the carbon capture process relative to the rate of liquid product formation. For cost-effective industrial separation of gases, pressure swing adsorption is a proven technology which has been proposed previously for the purification of electrolysis gases.[28,47] Pressure swing adsorption has been demonstrated for the separation of CO_2 from CO and other gases.[48] Table S3 (ESI†) contains capital expense information for a reference separation/recycle system from industry experience that was used to scale to the gaseous flow rates exiting the electrolyzers of the modeled CO_2 reduction processes.[28] The separation process was assumed to permit 97% of the CO_2 to be removed from the electrolyzer output and recycled back to the input with negligible concentrations of CO, H_2, or C_2H_4. For the cascade CO_2–CO–C_2H_5OH scenario, a pressure swing adsorption system of similar parameters was assumed feasible for the separation and recycle of CO back to the second electrolyzer.

Fischer–Tropsch system

In the first scenario, the CO_2–CO–FTL system, the CO product from electrolysis was combined with a separate H_2 stream to produce a syngas feedstock for the Fischer–Tropsch production of diesel fuel. Because the overall CO_2 reduction process is envisioned to be carbon-neutral or carbon-negative, the H_2 feedstock was assumed to come from clean-energy derived water electrolysis rather than conventional steam methane reforming. This led to a more expensive base case H_2 cost of \$5 kg^{-1} based on the H2A model for electrolysis.[45] Technoeconomic parameters for the rest of the Fischer–Tropsch process were drawn from a previous analysis for the conversion of coal to diesel fuel.[32] Although the syngas stoichiometric optimum H_2 : CO ratio is 2, the model Fischer–Tropsch system employed an iron catalyst which results in significant water–gas-shift activity which compensates for a suboptimal syngas composition. In the base case system, a syngas bypass unit maintained a H_2 : CO ratio of 1 entering the Fischer–Tropsch synthesis unit, as modeled for diesel fuel production.[32] Table S4 (ESI†) shows the breakdown of capital expenses and energy consumption by system component for the reference Fischer–Tropsch system, which was a coal-to-diesel + electricity process with recycle of unconverted syngas and venting of coproduct CO_2 (CTL–RC–V system).[32] However, this reference Fischer–Tropsch process contained numerous units necessary for the preparation of coal and for converting it to purified syngas. These components are not required in the CO_2–CO–FTL system employing a CO_2 electrolyzer to produce the purified CO feedstock. Only the system components downstream of the syngas feedstock were incorporated in the analysis, which included the Fischer–Tropsch island, the naphtha upgrading unit, the topping cycle in the power island, and the heat recovery plus steam cycle units.[32] In this reference Fischer–Tropsch system, after the desired diesel fuel product is separated, the remaining carbonaceous byproducts are combusted onsite for additional electricity production which was considered an electricity credit to offset electricity consumption in the rest of the CO_2–CO–FTL process. The electricity credit consisted of the steam turbine output plus export electricity minus the energy consumption of the recycle compressor and Fischer–Tropsch synthesis and refining units.[32] The base case Fischer–Tropsch conversion of CO to diesel fuel was 34% based on the reference system. For the sensitivity analysis on the effects of changes to the Fischer–Tropsch conversion rate, the resulting electricity generation from byproduct combustion was adjusted proportionately.

Electricity

A major contributor to the annual operating costs in each of the four scenarios was the cost of electricity to operate the CO_2 electrolyzers and other equipment. While the cost of electricity can vary by region, by source, and for residential *vs.* commercial applications, the base case average cost of electricity was assumed to be \$0.06 kWh^{-1}. This cost is on par with typical fossil-fuel derived electricity without carbon capture.[28,42,43,49] The added costs of carbon capture were included in the present analysis by explicitly accounting for the carbon capture capital expenses and adding the additional electricity consumption required to drive the carbon capture process to the annual operating expenses (Table S1, ESI†). The electricity costs for the production of hydrogen by electrolysis to provide the H_2 feedstock to the Fischer–Tropsch unit in the CO_2–CO–FTL system is implicit in the \$ kg^{-1} price of the H_2 and thus was not added to the annual electricity consumption. The use of solar photovoltaic and/or wind generated electricity to drive the CO_2 electrochemical reduction process would greatly contribute to the offsetting of greenhouse gas emissions, and the levelized cost of electricity from these renewable sources is increasingly competitive and in many regions already comparable to this base case fossil-fuel generated electricity price.[49]

Operating and maintenance

An annual operating and maintenance cost of 3.2% was applied for the electrolyzer installed capital cost based on previous analyses of PEM electrolysis.[42,45,46] The same rate was applied to the total capital expense of the carbon capture, gas separation, and Fischer–Tropsch systems as well to account for their operating and maintenance costs.

Byproduct value

With less than perfect faradaic efficiency for the electrochemical reduction of CO_2 to the desired product, significant byproduct output streams were produced. In the CO_2–CO–FTL process, these byproducts are combusted in the Fischer–Tropsch energy recovery unit to provide the electricity credit. In the other processes, particularly for the synthesis of ethanol which has notably lower faradaic efficiency, these byproducts have value which may lower the LCF value of the targeted liquid product. The significant byproducts include hydrogen, carbon monoxide, ethylene, and acetic acid and are assumed to be sold at the base case market values listed in Table S5 (ESI†).

Carbon credits

The electrochemical reduction of CO_2 to useful fuels and chemicals has the environmental appeal of reducing greenhouse gas emissions. If a policy is in place invoking a tax on carbon emissions, as has been proposed by many governments around the world, this reduction in CO_2 emissions would have financial value. The value of the CO_2 abatement in these processes could also be monetized under a cap and trade scheme in which the electrochemical CO_2 reduction facility could trade carbon credits to other industries. At present there is no national emissions tax or trading scheme in the United States, and the barrier to implementing one may remain high for the near term. As such, the base case scenarios in this analysis were conservative and assumed a zero dollar value per metric ton of CO_2 sequestered into useful products. For the sensitivity analysis, however, the high performance value assumed a fairly high value of \$100 per metric ton of CO_2. The annual mass of CO_2 sequestered in each process was determined based on the liquid product and byproduct molar flow rates and the respective number of carbons in each product. This carbon credit was taken as an offset to the annual operating costs.

Results and discussion

Following the methodology outlined above, each of the four scenarios for electrochemical reduction of CO_2 to liquid products was analyzed for its technoeconomic viability. In each case, a general process flow diagram is presented with the molar flow rates calculated according to the base case assumptions. These values were then used to determine the capital costs, operating costs, and product revenue, which was subsequently used to determine the LCF of the respective liquid product following eqn (3). The relevant base case parameters for each scenario are tabulated in the ESI.† Sensitivity analyses for each of the four processes were conducted to evaluate the effects of changes to the most important system parameters. For each parameter, this analysis assumed a high performance condition based on an aspirational but feasible value, as well as a corresponding low performance condition. The sensitivity analysis plots display the effects of each individual parameter change to the resulting calculation of the base case LCF. To get a sense of the possible cost reductions with a combination of system improvements for each CO_2 electroreduction process, a set of optimistic performance parameters were applied simultaneously, and the resulting optimistic LCF is compared to the base case value. This optimistic set of values was then further modified by assuming a favorable policy environment with a monetary value for the carbon emissions offset by the process.

CO_2 to CO to Fischer–Tropsch diesel

The base case along with the high and low performance parameters for the CO_2–CO–FTL system are shown in Table 2. Fig. 2 shows the system schematic with the corresponding molar flow rates that resulted from the base case assumptions. Note that the diesel fuel output from the Fischer–Tropsch process, which realistically consists of a mixture of mostly saturated hydrocarbons, was approximated as $C_{10}H_{22}$ for the determination of the molar flow rate. Base case conditions assume a state-of-the-art electrolyzer for the formation of CO, as has been demonstrated with Ag catalysts in ionic liquid electrolyte.[14] The base case Fischer–Tropsch conversion of CO to liquid product was 34% following the reference scenario.[32] However, under certain conditions this conversion rate has been reported at 80% or even higher,[28,31,32] hence the large improvement assumed for the high performance condition of Table 2. The capital cost multiplier parameters assume an overall reduction or increase in the total capital expense of the associated system component. The other CO_2–CO–FTL system values are reported in Table S6 (ESI†).

The base case parameters resulted in an LCF for diesel fuel of \$18.9 gge^{-1} (gallon of gas equivalent) for the CO_2–CO–FTL system. This cost is significantly higher than reported in a preceding analysis,[28] owing primarily to the higher assumed capital cost for the electrolyzers, along with more minor effects such as inflation. Fig. 3 shows the sensitivity analysis to the high and low performance parameters and how they would affect the resulting LCF for diesel fuel relative to the range of commercial diesel fuel costs. Across the US, the commercial price for diesel fuel varies by time and by region but has maintained a recent range of ~\$2.40–3.60 gal^{-1}.[50] Accounting for the difference of energy density between diesel and gasoline, this commercial fuel price is ~\$2.12–3.19 gge^{-1}. Thus, the base case scenario would not be economically competitive without improvements.

Among the modeled sensitivity parameters, the possible increase in the Fischer–Tropsch conversion efficiency produced the greatest decrease in the diesel LCF, decreasing to \$8.5 gge^{-1} for the high performance case. The high performance scenario envisioned sustained conversion rates at the high end of reported research results, leading to a large increase over the base case value from the reference Fischer–Tropsch study. Increasing the Fischer–Tropsch conversion is critical to lowering costs because it results in more diesel fuel produced per CO_2 treated, which leads to amortizing the capital costs over a greater amount of

Table 2 CO_2–CO–FTL system base case parameters and high and low performance parameters for the sensitivity analysis

	High performance	Base case	Low performance
CO_2 electrolysis cell voltage, V	1.5	1.8	2.1
CO_2 electrolysis current density, mA cm^{-2}	600	400	250
CO faradaic efficiency, %	98	98	75
Electrolyzer single-pass CO_2 conversion, %	75	50	25
Electrolyzer cost (uninstalled), \$ m^{-2}	15 464	30 927	46 391
Fischer–Tropsch conversion to fuel, %	80	34	34
Capital cost multiplier, CO_2 capture	0.5	1	1.5
Capital cost multiplier, CO_2/CO separation	0.5	1	1.5
Capital cost multiplier, Fischer–Tropsch	0.5	1	1.5
Cost of electricity, \$ kWh^{-1}	0.03	0.06	0.09
Cost of H_2, \$ kg^{-1} H_2	3	5	5
Fischer–Tropsch H_2 : CO ratio	1	1	2
Carbon emission cost, \$ per tonne CO_2	100	0	0

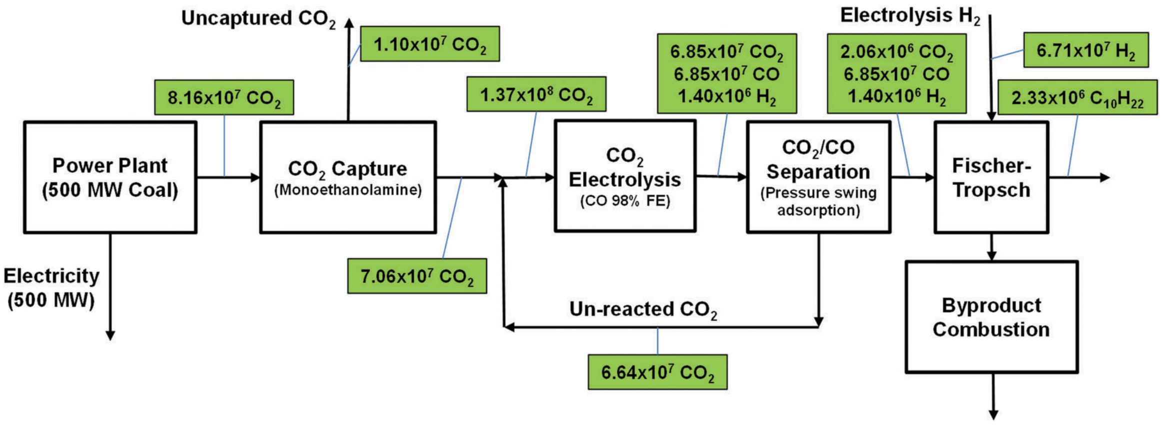

Fig. 2 Mass flow diagram for the CO_2–CO–FTL system under the base case parameters. Flow rates for each species (green boxes) are all reported in units of kmol yr^{-1}.

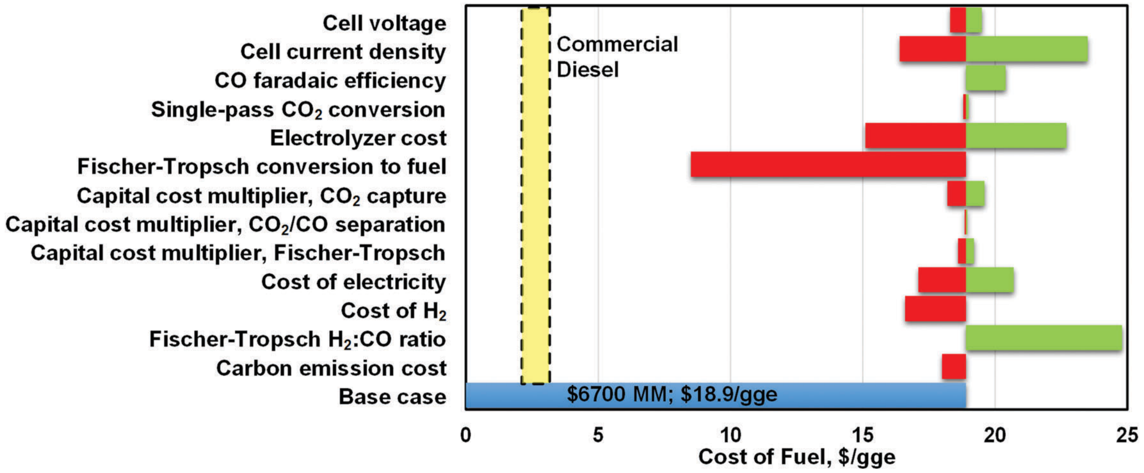

Fig. 3 Sensitivity analysis for the CO_2–CO–FTL case with parameters at the high (red bars) and low (green bars) performance conditions.

liquid product. In contrast, the single-pass conversion of CO_2 to CO in the electrolyzer had little effect on the resulting LCF because the separation and recycle process for CO_2 downstream of the electrolyzer already ensures that most of the CO_2 is ultimately converted. Similarly, the CO_2 capture, separations, and Fischer–Tropsch systems together accounted for only 20% of the total base case capital expense, and thus modifications to these capital costs did not result in major changes to the diesel LCF.

Modifications to the electrolyzer parameters are the next considerable opportunity for lowering costs in the CO_2–CO–FTL system. Although reducing the cell voltage lowered the LCF by reducing the electricity consumption, the electrolyzer current density and capital cost per electrode area were more significant factors. Increased current density means that less total electrode area is required for a given CO production rate, which would reduce the electrolyzer capital cost. Similarly, reductions in the electrolyzer cost per electrode area, through benefits of manufacturing at high scale or by significant design improvements, lead to direct savings in the electrolyzer capital costs which made up 80% of the total base case capital expense (Table S6, ESI†). A high faradaic efficiency of the desired product is likewise vital to maximizing the value of the electrolyzer capital investment, but in the CO_2–CO–FTL case (98% FE) there is negligible room for improvement. At a low performance condition of 75% FE, the LCF was projected to increase by \$1.5 gge^{-1}, indicating the importance of maintaining high selectivity in the electrochemical reduction. The cost of electricity was also an important variable. Both electrolysis and CO_2 capture are energy-intensive processes, resulting in significant energy consumption for the CO_2–CO–FTL system. However, a large decrease in the price of electricity would be difficult and require improvements across a major industry. Increases from the base case cost per kWh, however, are easily conceivable, particularly if primarily fossil-fuel-free power sources are leveraged such as renewables backed up by energy storage. At \$0.09 kWh^{-1}, the base case LCF of diesel increased by \$1.8 gge^{-1}. Another major contributor to the operating costs in the CO_2–CO–FTL system is the price of hydrogen needed to blend the CO electrolysis product into syngas for Fischer–Tropsch conversion. At a reduced cost of \$3 kg^{-1} for clean H_2, the diesel LCF decreased by \$2.3 gge^{-1}. Also, the base case assumes that a 1 : 1 H_2 : CO ratio is sufficient for diesel production, but in a low performance case where conditions instead require the stoichiometric optimum ratio of 2 : 1, the LCF suffered a significant increase of \$5.9 gge^{-1}. Thus, maintaining the Fischer–Tropsch catalyst and reactor for efficient performance with less hydrogen is vital to the system cost. It is also possible to eliminate the need for a separate clean H_2 feedstock by intentionally running the CO_2 electrolyzer at conditions which are more favorable for hydrogen evolution. If the CO faradaic efficiency of the electrolyzer is reduced to 50% with the balance directed to water-splitting, H_2 and CO would be co-evolved at the requisite ratio for the Fischer–Tropsch conversion. Such a condition leads to zero additional hydrogen feedstock required. However, the co-evolution of the syngas components was actually projected to increase the diesel LCF to a total of \$23.7 gge^{-1}. Co-evolution of H_2 and CO did not reduce costs because the same total current must be passed to generate the same molar flow rate of syngas. Co-evolution of hydrogen in the CO_2 electrolyzer forces H_2 to be produced at a lower operating current density than is achievable by commercial PEM water electrolyzers, and thus leads to greater capital expense and more expensive hydrogen. However, controlled electrolysis co-evolution of H_2 with CO could be beneficial for rapid modification of the H_2 : CO syngas ratio as needed in real time for the control of the Fischer–Tropsch process.[51]

At a base case cost of \$18.9 gge^{-1}, simultaneous improvements across many system parameters would be needed to increase the likelihood of the economic competitiveness of the CO_2–CO–FTL system. The base case conditions are compared in Table 3 to a collection of favorable parameters which constitute an optimistic scenario. As shown in Fig. 4, together these conditions led to an optimistic case LCF for diesel fuel of \$4.4 gge^{-1}, placing the process far closer to commercial viability. If the carbon emission cost benefit of \$100 per tonne CO_2 is applied as well, the cost of diesel fuel was reduced to \$3.5 gge^{-1}. Even at this

Table 3 CO_2–CO–FTL system base case and optimistic case parameters

	Base case	Optimistic case
CO_2 electrolysis cell voltage, V	1.8	1.5
CO_2 electrolysis current density, mA cm^{-2}	400	600
CO faradaic efficiency, %	98	98
Electrolyzer single-pass CO_2 conversion, %	50	75
Electrolyzer cost (uninstalled), \$ m^{-2}	30 927	15 464
Fischer–Tropsch conversion to fuel, %	34	80
Capital cost multiplier, CO_2 capture	1.0	1.0
Capital cost multiplier, CO_2/CO separation	1.0	1.0
Capital cost multiplier, Fischer–Tropsch	1.0	1.0
Cost of electricity, \$ kWh^{-1}	0.06	0.03
Cost of H_2, \$ kg^{-1} H_2	5	3
Fischer–Tropsch H_2 : CO ratio	1	1
Carbon emission cost, \$ per tonne CO_2	0	0

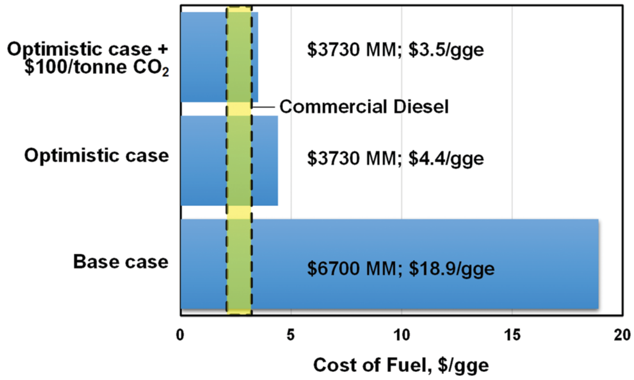

Fig. 4 CO_2–CO–FTL system capital costs and fuel cost per gallon of gas equivalent (gge) for the base case, the optimistic case, and the optimistic case with an added carbon tax.

ambitious cost for CO_2, the greenhouse gas offset benefit did little to reduce the LCF from the base case conditions (Fig. 3). However, as the LCF decreases, the economic benefit of a price for carbon emissions becomes more significant and could make the difference between a viable technology and an impractical one.

CO_2 to C_2H_5OH

The electrochemical reduction of CO_2 to ethanol was analyzed through two possible routes, one utilizing a direct single-step electrolysis (CO_2–C_2H_5OH) and another leveraging a two-stage cascade electrolysis (CO_2–CO–C_2H_5OH). Fig. 5 shows the process schematic and molar flow rates for the CO_2–C_2H_5OH process under the base case conditions of Table 4. The CO_2–C_2H_5OH base case assumed a state-of-the-art electrolyzer for the direct synthesis of ethanol from CO_2, which was based on the highest performing operating point for a reactor with a nanostructured Cu wire mesh cathode.[27] This cell achieved a C_2H_5OH faradaic efficiency up to ~28% at high current density and is among the best reported results for electrochemical ethanol production. For the high performance condition for the one-step electroreduction of CO_2 to C_2H_5OH, a faradaic efficiency for ethanol as high as 63% has been reported.[38] This value was not assumed for the base case CO_2–C_2H_5OH parameter since it is notably higher than other state-of-the-art ethanol-selective catalysts and was achieved at ~2 mA cm^{-2}. Accomplishing this faradaic efficiency at the other base case parameters thus represents an aspirational goal for a high performance system. The current that does not lead to ethanol formation instead produces ethylene, hydrogen, and carbon monoxide.[27] These byproducts were assumed to be sold at the base case market prices of Table 4 and added to the annual product revenue. The other CO_2–C_2H_5OH system values are reported in Table S7 (ESI†).

The single-step CO_2–C_2H_5OH base case parameters resulted in an untenably high LCF for ethanol of \$55.3 gge^{-1}. Recent prices for ethanol have fluctuated between ~\$1.40–1.70 gal^{-1}, which is ~\$2.10–2.55 gge^{-1}. Clearly then, the single-step electrochemical reduction of CO_2 to ethanol requires major improvements from the base case conditions to have any chance of economic competitiveness. Using the high and low performance conditions of Table 4, the sensitivity to the ethanol LCF is shown in Fig. 6. For the CO_2–C_2H_5OH system, the same general trend was evident in the magnitude of the effect each parameter had on the LCF as described above for the CO_2–CO–FTL system. The single-pass CO_2 conversion and the capital costs for CO_2 capture and separation processes were not significant factors. Fluctuations to the market price of ethylene and hydrogen made little difference, while the price of carbon monoxide was moderately more important since it was produced in higher mass. The cost of electricity was again significant, with the energy to

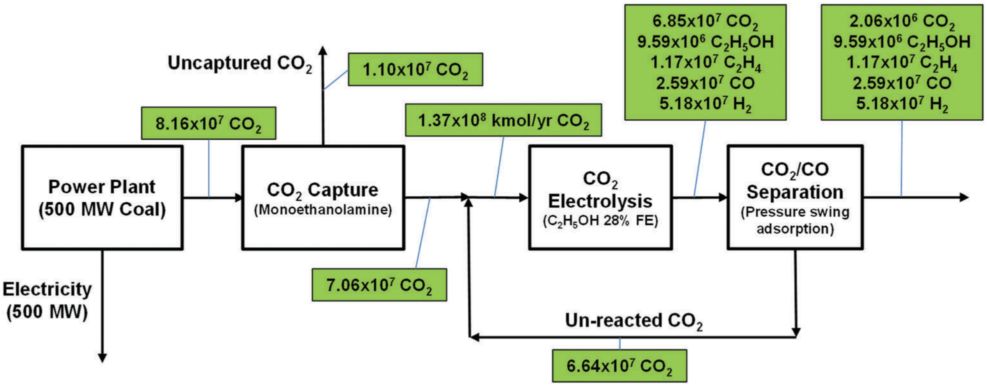

Fig. 5 Mass flow diagram for the CO_2–C_2H_5OH system under the base case parameters. Flow rates for each species (green boxes) are all reported in units of kmol yr^{-1}.

Table 4 CO_2–C_2H_5OH system base case parameters and high and low performance parameters for the sensitivity analysis

	High performance	Base case	Low performance
CO_2 electrolysis cell voltage, V	2.0	2.3	2.6
CO_2 electrolysis current density, mA cm^{-2}	350	250	150
C_2H_5OH faradaic efficiency, %	63	28	15
Electrolyzer single-pass CO_2 conversion, %	75	50	25
Electrolyzer cost (uninstalled), \$ m^{-2}	15 464	30 927	46 391
Capital cost multiplier, CO_2 capture	0.5	1.0	1.5
Capital cost multiplier, CO_2/CO separation	0.5	1.0	1.5
Cost of electricity, \$ kWh^{-1}	0.03	0.06	0.09
Price of ethylene, \$ kg^{-1}	1.19	0.99	0.79
Price of hydrogen, \$ kg^{-1}	2.30	1.90	1.50
Price of carbon monoxide, \$ kg^{-1}	0.80	0.60	0.40
Carbon emission cost, \$ per tonne CO_2	100	0	0

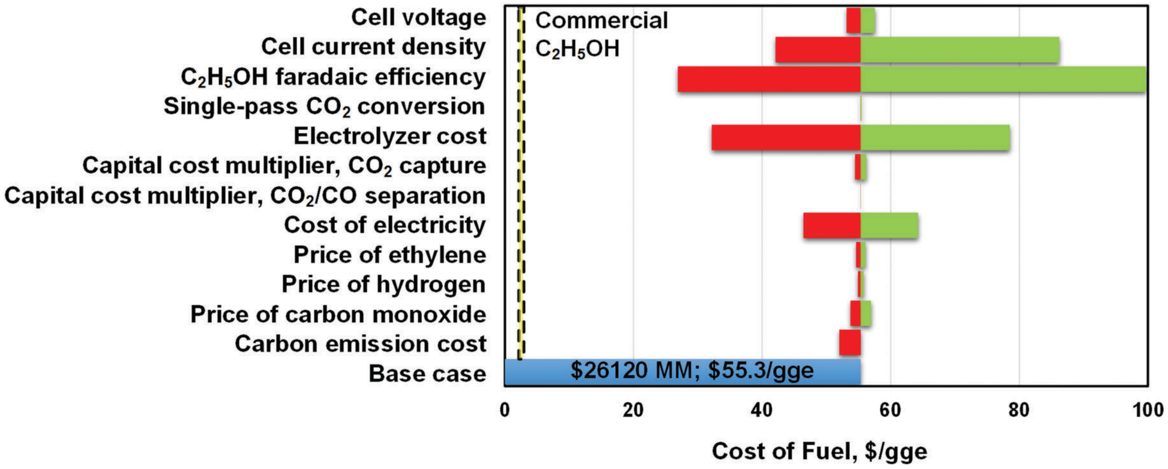

Fig. 6 Sensitivity analysis for the CO_2–C_2H_5OH case with parameters at the high (red bars) and low (green bars) performance conditions.

run the electrolyzer constituting ~95% of the electricity consumption. Thus, a reduction in the electrolyzer cell voltage consequently leads to significant electricity savings which has a modest impact on the LCF.

However, by far the most important parameters for reducing the LCF of ethanol were the system variables which can affect the electrolyzer capital cost per gge of C_2H_5OH produced. In the single-step CO_2–C_2H_5OH base case, the electrolyzer system accounted for 96% of the total capital expense, making it the most important factor in high ethanol cost. Thus, an increase in the current density from 250 to 350 mA cm^{-2} and the subsequent electrolyzer capital savings led to a decrease in the LCF of \$13.3 gge^{-1}. Similarly, cutting the capital cost per electrode area in half reduced the LCF by \$23.2 gge^{-1}. Unlike the CO_2–CO–FTL system in which the electrolysis faradaic efficiency is already nearly ideal, the CO_2–C_2H_5OH base case FE leaves much room for improvement. Indeed, if the highest reported literature FE of 63% were achievable at the other system parameters, a decrease in the ethanol cost by \$28.5 gge^{-1} was predicted. Increased ethanol faradaic efficiency leads to lower required electrode area with the additional benefit of less electricity consumption directed toward byproduct formation. Faradaic efficiency was thus a critical metric for the CO_2–C_2H_5OH system, and a modest decrease to 15% for the low performance condition (still higher than most electrochemical ethanol production reports) led to an extreme increase in the LCF to a total value of \$99.7 gge^{-1}.

Table 5 lists the CO_2–C_2H_5OH optimistic case values which led to the ethanol LCF and capital costs shown in Fig. 7. A combination of increased faradaic efficiency and current density with lower capital cost per electrode area, as well as the less significant system improvements, reduced the total capital expense by 55% and reduced the LCF to \$10.1 gge^{-1}. The addition of a \$100 per tonne CO_2 emission credit reduced this further to \$8.6 gge^{-1}. This result is a drastic improvement from the base case ethanol price, but it is still much too expensive for economic

Table 5 CO_2–C_2H_5OH system base case and optimistic case parameters

	Base case	Optimistic case
CO_2 electrolysis cell voltage, V	2.3	2.0
CO_2 electrolysis current density, mA cm^{-2}	250	300
C_2H_5OH faradaic efficiency, %	28	63
Electrolyzer single-pass CO_2 conversion, %	50	75
Electrolyzer cost (uninstalled), \$ m^{-2}	30 927	15 464
Capital cost multiplier, CO_2 capture	1.0	1.0
Capital cost multiplier, CO_2/CO separation	1.0	1.0
Cost of electricity, \$ kWh^{-1}	0.06	0.03
Price of ethylene, \$ kg^{-1}	0.99	1.09
Price of hydrogen, \$ kg^{-1}	1.90	2.00
Price of carbon monoxide, \$ kg^{-1}	0.60	0.70
Carbon emission cost, \$ per tonne CO_2	0	0

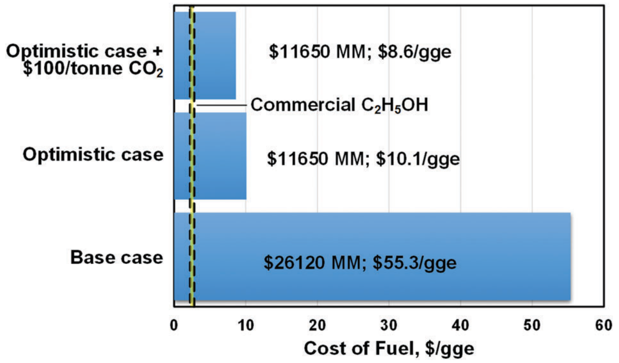

Fig. 7 CO_2–C_2H_5OH system capital costs and fuel cost per gallon of gas equivalent (gge) for the base case, the optimistic case, and the optimistic case with an added carbon tax.

viability relative to present ethanol commercial prices. Furthermore, if the optimistic conditions are improved to an impractical dream scenario by employing a one-step CO_2-to-ethanol faradaic efficiency of 100%, the LCF for ethanol decreases to \$8.1 gge^{-1} (and to \$7.1 gge^{-1} with \$100 per tonne CO_2) which is still significantly greater than the commercial price.

As an alternative to the one-step conversion of CO_2 to ethanol, a two-step electrochemical cascade route can leverage the low voltage, high faradaic efficiency synthesis of CO and subsequent high selectivity conversion of CO to ethanol to achieve higher total system performance. Fig. 8 shows the process schematic and molar flow rates of the CO_2–CO–C_2H_5OH system under the base case parameters of Table 6. The base case CO_2–CO–C_2H_5OH parameters again assume state-of-the-art electrolyzers, with the same high performance Ag catalyst conditions for CO electrosynthesis[14] used in the CO_2–CO–FTL case coupled with an optimized secondary CO electrolyzer using an oxide-derived Cu cathode for conversion to ethanol.[39] Faradaic efficiency for the electroreduction of CO to C_2H_5OH was reported as high as 45%, with byproducts of ethylene, acetic acid, and hydrogen. The reported CO reduction cell relied on the diffusion of dissolved CO, and thus due to the low solubility of CO the measured system current density was low.[39] The base case technoeconomic parameters for CO electrolysis instead assume a more optimized design employing gaseous CO fed through a catalyst-decorated gas diffusion electrode, an approach which has consistently demonstrated higher electroreduction current density by mitigating mass transport limitations.[26,41] Otherwise, capital cost

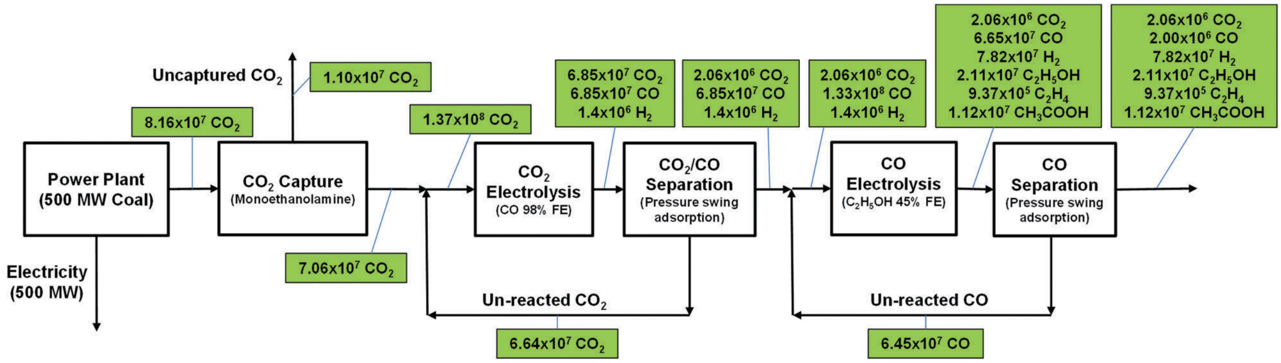

Fig. 8 Mass flow diagram for the CO_2–CO–C_2H_5OH system under the base case parameters. Flow rates for each species (green boxes) are all reported in units of kmol yr^{-1}.

Table 6 CO_2–CO–C_2H_5OH system base case parameters and high and low performance parameters for the sensitivity analysis

	High performance	Base case	Low performance
CO_2 electrolysis cell voltage, V	1.5	1.8	2.1
CO_2 electrolysis current density, mA cm^{-2}	600	400	250
CO faradaic efficiency, %	98	98	75
Electrolyzer single-pass CO_2 conversion, %	75	50	25
CO_2 electrolyzer cost (uninstalled), \$ m^{-2}	15 464	30 927	46 391
CO electrolysis cell voltage, V	1.6	1.9	2.2
CO electrolysis current density, mA cm^{-2}	300	120	60
C_2H_5OH faradaic efficiency, %	60	45	30
Electrolyzer single-pass CO conversion, %	75	50	25
CO electrolyzer cost (uninstalled), \$ m^{-2}	15 464	30 927	46 391
Capital cost multiplier, CO_2 capture	0.5	1.0	1.5
Capital cost multiplier, separation	0.5	1.0	1.5
Cost of electricity, \$ kWh^{-1}	0.03	0.06	0.09
Price of ethylene, \$ kg^{-1}	1.19	0.99	0.79
Price of hydrogen, \$ kg^{-1}	2.30	1.90	1.50
Price of carbon monoxide, \$ kg^{-1}	0.80	0.60	0.40
Price of acetic acid, \$ kg^{-1}	0.80	0.60	0.40
Carbon emission cost, \$ per tonne CO_2	100	0	0

calculations for CO electrolysis and gas separation were analyzed identically to CO_2 electrolysis. The other CO_2–CO–C_2H_5OH system values are reported in Table S8 (ESI†).

The base case parameters for the two-step electrosynthesis of ethanol led to an LCF of \$49.8 gge^{-1}, which was lower than the base case one-step CO_2–C_2H_5OH but still far higher than the commercial price of ethanol. The total two-step CO_2–CO–C_2H_5OH capital expense was more than double that of the base case one-step CO_2–C_2H_5OH, but this cost was offset by more than doubling the ethanol molar production rate. Notably, however, the cascade electrolysis approach does not fundamentally require an increase in the electrolyzer capital expense. If the CO_2-to-CO and CO-to-C_2H_5OH electrolyzers operated at the same current density and faradaic efficiencies as a one-step CO_2-to-C_2H_5OH electrolyzer, the same total electrode area and electrolyzer capital cost would result because both approaches require 12 electrons to convert CO_2 to C_2H_5OH. Only the additional gas separation and recycle step would increase the capital expense in this case for the two-step synthesis, but the gas separation capital cost was negligible compared to the electrolyzer capital cost (Table S8, ESI†).

The high and low performance conditions of Table 6 for the two-step electrosynthesis were used to produce the sensitivity analysis shown in Fig. 9. Similar trends were observed as seen in the previous cases, with minor effects from the non-electrolyzer capital costs, the byproduct prices, and the single-pass reactor conversion. The cost of electricity had a modest effect, increasing or decreasing the LCF by \$4.1 gge^{-1}. Again, the electrolyzer parameters had the greatest effect. However, modifications to the cell 1 (CO_2-to-CO) conditions had far less impact than changes to cell 2 (CO-to-C_2H_5OH). The cell 1 parameters had less effect on the ethanol LCF because the faradaic efficiency and current density were already quite high compared to cell 2 and only one third of the electrons directly contributing to the synthesis of ethanol must be passed in the first electrolyzer. As a consequence, the base case capital expense of the CO electrolyzers was 8.9 times greater than the capital expense of the CO_2 electrolyzers (Table S8, ESI†). Thus, parameters which affected the second electrolyzer capital cost (*i.e.*, current density, faradaic efficiency, and electrolyzer cost per area) had by far the greatest sensitivity on the resulting LCF. Increasing the ethanol faradaic efficiency decreases the electrolyzer 2 capital while simultaneously reducing the electricity directed to byproducts, and the high performance increase to 60% FE led to a decrease in the LCF of \$11.1 gge^{-1}. Increasing the cell 2 current density led to the largest ethanol cost reduction, a \$24.0 gge^{-1} decrease, which reinforces the importance of electrolyzer design to maximize mass transport of the reactant to the catalyst interface.

Table 7 lists the CO_2–CO–C_2H_5OH optimistic case values which led to the ethanol LCF and capital costs shown in Fig. 10. Like the one-step ethanol electrosynthesis, increased faradaic efficiency and current density with lower capital cost per electrode area led to major cost savings. The optimistic case lowered the total capital expense by 78% and reduced the LCF to \$8.2 gge^{-1}. Under the optimistic scenario, the total capital expense for the two-step CO_2–CO–C_2H_5OH electrosynthesis was only ~1% higher than the capital expense of the one-step CO_2–C_2H_5OH, which shows that the cascade approach can be competitive in terms of capital expenditure. Applying the additional carbon emissions offset of \$100 per tonne CO_2 to the optimistic case resulted in \$6.9 gge^{-1}. If the optimistic conditions are improved to a dream scenario by employing a CO-to-ethanol faradaic efficiency of 100%, the LCF for ethanol decreases to \$6.7 gge^{-1} (and to \$5.7 gge^{-1} with \$100 per tonne CO_2) which is still significantly greater than the commercial price. Thus, while the

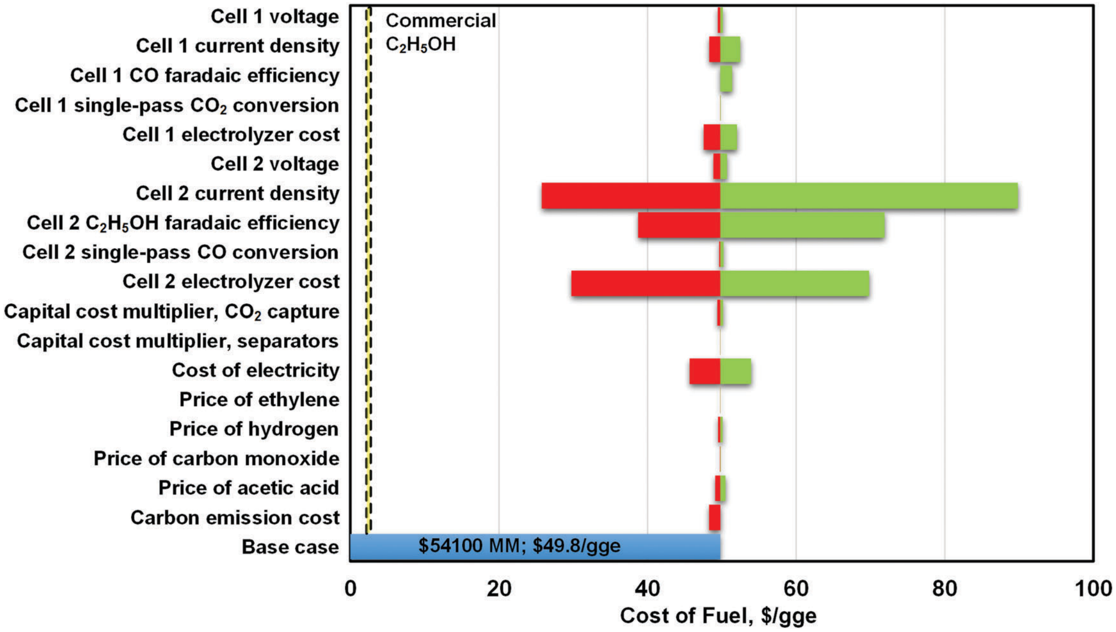

Fig. 9 Sensitivity analysis for the CO_2–CO–C_2H_5OH case with parameters at the high (red bars) and low (green bars) performance conditions.

Table 7 CO_2–CO–C_2H_5OH system base case and optimistic case parameters

	Base case	Optimistic case
CO_2 electrolysis cell voltage, V	1.8	1.5
CO_2 electrolysis current density, mA cm^{-2}	400	600
CO faradaic efficiency, %	98	98
Electrolyzer single-pass CO_2 conversion, %	50	75
CO_2 electrolyzer cost (uninstalled), \$ m^{-2}	30 927	15 464
CO electrolysis cell voltage, V	1.9	1.6
CO electrolysis current density, mA cm^{-2}	120	300
C_2H_5OH faradaic efficiency, %	45	60
Electrolyzer single-pass CO conversion, %	50	75
CO electrolyzer cost (uninstalled), \$ m^{-2}	30 927	15 464
Capital cost multiplier, CO_2 capture	1.0	1.0
Capital cost multiplier, separation	1.0	1.0
Cost of electricity, \$ kWh^{-1}	0.06	0.03
Price of ethylene, \$ kg^{-1}	0.99	1.09
Price of hydrogen, \$ kg^{-1}	1.90	2.00
Price of carbon monoxide, \$ kg^{-1}	0.60	0.70
Price of acetic acid, \$ kg^{-1}	0.60	0.70
Carbon emission cost, \$ per tonne CO_2	0	0

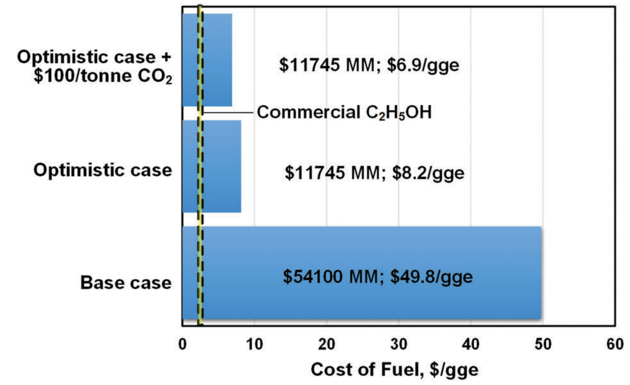

Fig. 10 CO_2–CO–C_2H_5OH system capital costs and fuel cost per gallon of gas equivalent (gge) for the base case, the optimistic case, and the optimistic case with an added carbon tax.

two-step cascade electrochemical synthesis was projected to result in a cheaper ethanol LCF than the one-step method, both approaches would require major advancements in both selectivity and current density to have any chance of commercial viability.

CO_2 to HCOOH

Formic acid was the final liquid product of electrochemical CO_2 reduction analyzed for technoeconomic feasibility. HCOOH is a stable, low volatility liquid at room temperature (vapor pressure of 40 mmHg at 20 °C). While not as energy dense as diesel fuel or ethanol, HCOOH has shown promise as a basis for a hydrogen storage technology (53.4 g H_2 L^{-1} at ambient temperature and pressure).[52–54] Fig. 11 shows the process schematic and molar flow rates for the CO_2–HCOOH system as calculated from the base case parameters listed in Table 8. The base case electrolyzer conditions were based on a state-of-the-art formic acid reactor utilizing a nanoparticle Sn catalyst-based gas diffusion electrode as the cathode with a novel multicomponent ion exchange membrane.[41] A stable HCOOH faradaic efficiency as high as 94% was reported at 140 mA cm^{-2}, although the required cell voltage was high compared to the other systems at 3.5 V. The other CO_2–HCOOH base case system values are given in Table S9 (ESI†).

The base case analysis resulted in an LCF for HCOOH of \$1.16 kg^{-1}, which accounting for the energy density of formic acid is equivalent to \$28.8 gge^{-1}.[54] Clearly, HCOOH produced at this price would not be economically competitive with petroleum-derived gasoline as a fuel. However, formic acid as a commodity chemical is sold in bulk at \$0.4–0.6 kg^{-1}. Thus, while the base case LCF for formic acid indicates it may not be easily viable as a fuel, electrochemical reduction of CO_2 to HCOOH could be close to economic competitiveness on the chemical market. Unlike the previous cases then, the LCF of HCOOH is reported in the sensitivity analysis and optimistic case in \$ kg^{-1} for comparison to this commercial price. From the high and low performance conditions of Table 8, a sensitivity analysis was conducted as shown in Fig. 12. As for the other systems, the effects of non-electrolyzer capital costs, byproduct prices, and CO_2 conversion rate were minor. The applied electrolysis cell voltage, despite being high in the CO_2–HCOOH case relative to the other processes, also did not have a large impact at the high and low performance values. Reducing the applied electrolysis potential only reduces costs by lowering the electricity consumption of the electrolyzers, and the 0.5 V decrease from the base case achieved in the high performance condition

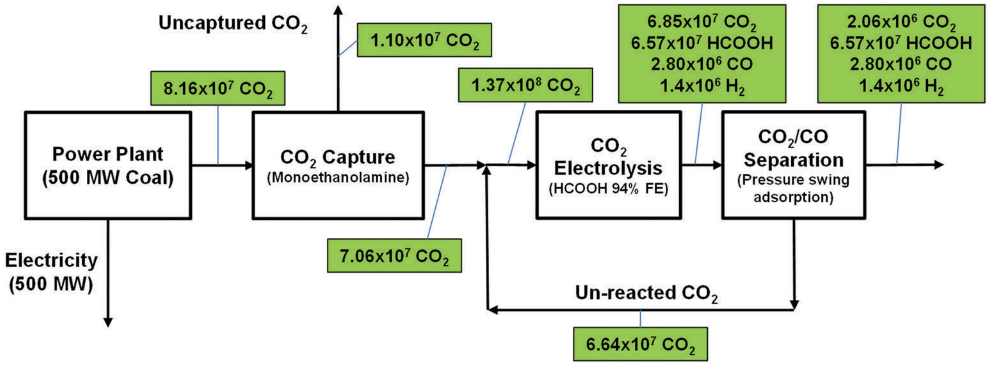

Fig. 11 Mass flow diagram for the CO_2–HCOOH system under the base case parameters. Flow rates for each species (green boxes) are all reported in units of kmol yr^{-1}.

Table 8 CO_2–HCOOH system base case parameters and high and low performance parameters for the sensitivity analysis

	High performance	Base case	Low performance
CO_2 electrolysis cell voltage, V	3.0	3.5	4.0
CO_2 electrolysis current density, mA cm^{-2}	210	140	70
HCOOH faradaic efficiency, %	98	94	75
Electrolyzer single-pass CO_2 conversion, %	75	50	25
Electrolyzer cost (uninstalled), \$ m^{-2}	15 464	30 927	46 391
Capital cost multiplier, CO_2 capture	0.5	1.0	1.5
Capital cost multiplier, CO_2/CO separation	0.5	1.0	1.5
Cost of electricity, \$ kWh^{-1}	0.03	0.06	0.09
Price of hydrogen, \$ kg^{-1}	2.30	1.90	1.50
Price of carbon monoxide, \$ kg^{-1}	0.80	0.60	0.40
Carbon emission cost, \$ per tonne CO_2	100	0	0

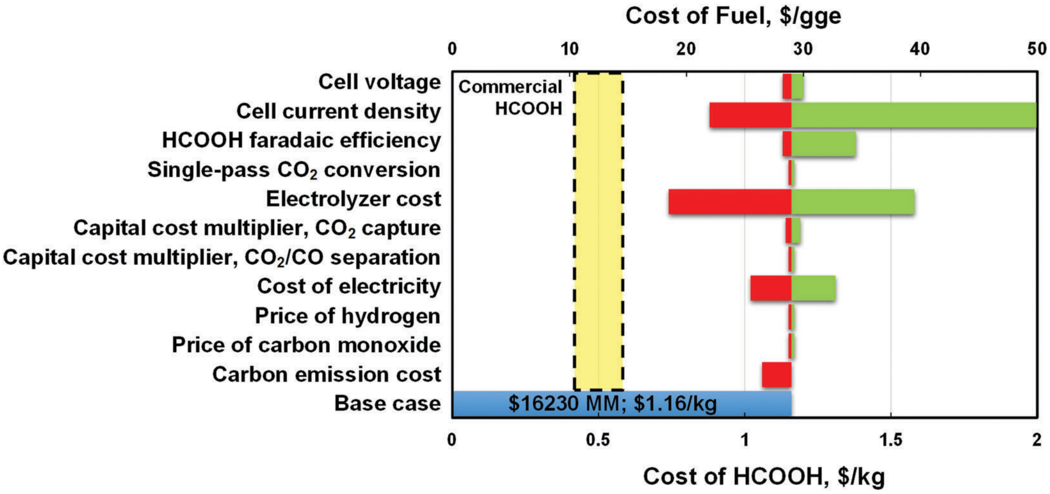

Fig. 12 Sensitivity analysis for the CO_2–HCOOH case with parameters at the high (red bars) and low (green bars) performance conditions. The commercial HCOOH price range of ~\$0.4–0.6 kg^{-1} is also outlined.

only reduced the total electricity consumption by 13%. As with the other scenarios, the capital expense of the electrolyzer units was projected to be the dominant cost. Thus, direct reductions in the cost per electrode area had a large effect, with a 50% reduction in \$ m^{-2} resulting in a concomitant drop in the LCF of \$0.42 kg^{-1}. At a base case 94% faradaic efficiency, there is little room for improvement, though a drop at low performance was again seen to correlate to a significant increase in the \$ kg^{-1} HCOOH. Current density was similarly important, with a 50% increase leading to a reduction in the LCF of \$0.28 kg^{-1}, and a 50% decrease leading to a large increase of \$0.84 kg^{-1} in the LCF. Maintaining high electrolysis current density is thus a critical metric for achieving economic viability.

Table 9 CO_2–HCOOH system base case and optimistic case parameters

	Base case	Optimistic case
CO_2 electrolysis cell voltage, V	3.5	3.2
CO_2 electrolysis current density, mA cm^{-2}	140	200
HCOOH faradaic efficiency, %	94	96
Electrolyzer single-pass CO_2 conversion, %	50	75
Electrolyzer cost (uninstalled), \$ m^{-2}	30 927	15 464
Capital cost multiplier, CO_2 capture	1.0	1.0
Capital cost multiplier, CO_2/CO separation	1.0	1.0
Cost of electricity, \$ kWh^{-1}	0.06	0.03
Price of hydrogen, \$ kg^{-1}	1.90	2.00
Price of carbon monoxide, \$ kg^{-1}	0.60	0.70
Carbon emission cost, \$ per tonne CO_2	0	0

Table 9 lists the CO_2–HCOOH optimistic case parameters which led to the formic acid levelized costs and total capital costs given in Fig. 13. At this set of optimistic conditions, the HCOOH cost was only \$0.46 kg^{-1}, placing it well within the range of commercial HCOOH prices. This benefit is due primarily to the assumed increase in current density and decrease in electrolyzer cost per area. Thus, with reactor design improvements to reach higher current densities and electrolyzer component cost reductions and benefits from commercial scaleup, the electrochemical reduction of CO_2 to HCOOH might be commercially feasible. Moreover, assuming the carbon emission cost of \$100 per tonne further lowered the cost to \$0.36 kg^{-1} HCOOH, which would be cheaper than the typical market price.

Prospects

The preceding analysis compared four possible routes for the electrochemical reduction of CO_2 to liquid products using one consistent technoeconomic methodology and current state-of-the-art assumptions for the various electrolysis conditions. Thus while practically achievable commercial values may deviate somewhat from the base case conditions, the trends in product cost and parameter sensitivity between the four systems are

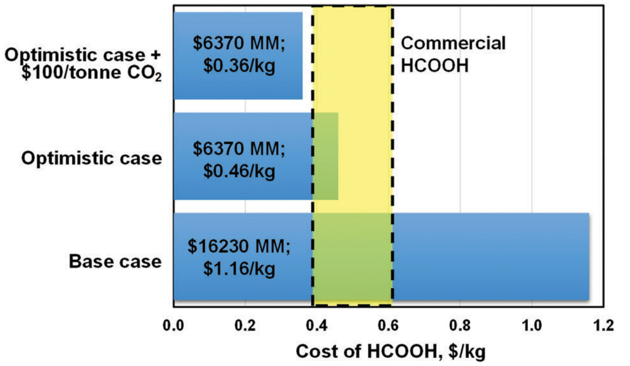

Fig. 13 CO_2–HCOOH system capital costs and cost of HCOOH per kg for the base case, the optimistic case, and the optimistic case with an added carbon tax.

indicative of the relative feasibility of these processes. In all four cases, it was seen that electrolyzer capital cost was a significant if not dominant factor. Therefore, efforts to increase the operating current density and reduce the electrolyzer cost per electrode area are critical. Pathways to accomplishing this include reactor design enhancements to increase the CO_2 mass flux to the catalyst interface and cheaper system components. Production of ion exchange membrane based electrolyzers at large scale may also help reduce capital costs. Achieving high product faradaic efficiency is also critical to minimizing capital costs and excess energy usage. In contrast, realistic decreases to the applied cell voltage were observed to affect only modest cost reductions, making this a secondary concern for achieving cost-effective CO_2 reduction. Thus, researchers of electrocatalysts for CO_2 reduction may find more practical benefit in focusing on increased product selectivity and current density even if higher overpotentials are required.

The projected LCFs for each of the four processes under the various cases are summarized in Fig. 14. In terms of producing a cost-effective liquid fuel *via* electrochemical CO_2 conversion, the CO_2–CO–FTL system showed the most promise with an optimistic case diesel LCF of \$4.4 gge^{-1}. However, this scenario required significant enhancement in the Fischer–Tropsch conversion rate as well as electrolyzer improvements. Ethanol production, through either one-step or two-step electrosynthesis, faces a daunting set of research challenges to approach cost-competitiveness. Chief among these are a need for strongly increased catalyst selectivity and higher current density. Formic acid, because of its relatively low energy density, likewise resulted in high costs per gallon of gasoline equivalent, making it impractical as a fuel. Nevertheless, the technoeconomic analysis indicates electrochemical synthesis of HCOOH may still be the most readily commercializable of the four processes since the optimistic case levelized cost of \$0.46 kg^{-1} HCOOH falls within the commercial price range. The preceding analysis, however, does not account for the market size. The market for fuels is enormous and unlikely to constrain the analysis, but the market for formic acid as a chemical is far smaller and may affect the economics at production scales as high as the basis used in this work. Cost-effective production of HCOOH at relatively small scale for the chemical market may still represent one of the most promising methods for electrochemical CO_2 reduction to achieve a foothold in industry. Furthermore, for each of the four processes, the carbon emission credit in relation to the amount of CO_2 sequestered had little effect under the base case conditions but became increasingly significant at the lower levelized costs of the optimistic scenarios. For a CO_2 electroreduction technology on the edge of economic competitiveness, a societal carbon emission cost policy could thus make the difference for viability.

Additionally, alternative sources for a CO_2 feedstock besides power plant post-combustion exhaust are conceivable. The large, industrially relevant processes of fermentation,[55,56] aluminum refining,[57,58] and cement manufacture[59] are all major emitters of CO_2 in high concentration streams which could be harnessed as a feedstock for electroreduction to fuels. However, the sensitivity analyses presented above for all four scenarios indicate that the effects of the carbon capture process, through both capital and operating expenses, are minimal to the final base case LCF value. Thus, the ability of alternative CO_2 sources to improve the technoeconomic outlook for the electroreduction of CO_2 to liquid products is expected to be minor.

Finally, it must be recognized that an electrochemical CO_2 reduction process only makes sense environmentally if the energy driving the conversion is carbon-free or carbon-neutral. Thermodynamics would suggest that reducing CO_2 will require more energy input than can be harvested during the combustion which produced the CO_2. Indeed, for all four systems the total electrolyzer power requirement was greater than the 500 MW output of the fossil-fuel-based power plant creating the CO_2 feedstock (Tables S6–S9, ESI†). If fossil-fuel derived electricity was used to drive the electrolysis, the net result would thus be an increase in CO_2 emissions. Clean power sources such as wind and solar would be needed to drive the electrolysis, although full treatment of a fossil fuel power plant exhaust would require an even larger renewable energy utility. Moreover, the intermittency of wind and solar mean that these sources have a reduced capacity factor which was not accounted for in the preceding analysis. Photovoltaics have a capacity factor of approximately 20%.[42]

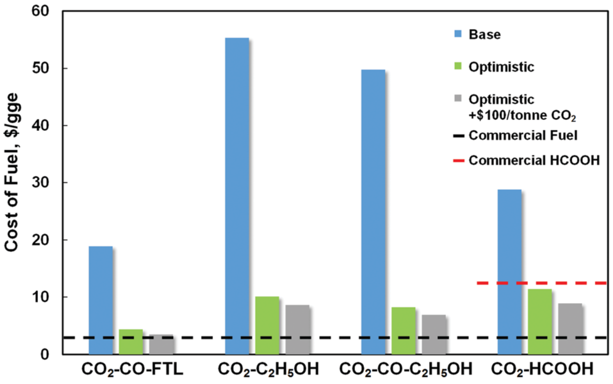

Fig. 14 Projected levelized cost of fuel summary for the four processes for their respective base, optimistic, and optimistic + \$100 per tonne CO_2 cases.

Renewable electricity sources backed up by clean energy storage technologies would therefore be required to ensure that the CO_2 electrolyzer capital equipment could run at full capacity. While this would likely lead to higher electricity costs and consequently higher levelized fuel costs than the base case modeled here, the cost of electricity was observed in each case to be only a modestly sensitive variable compared to the electrolyzer parameters.

Conclusions

Four possible routes for the electrochemical conversion of power plant flue gas CO_2 to liquid products were analyzed for techno-economic viability. A high efficiency electrolysis to CO coupled with Fischer–Tropsch conversion to diesel fuel seems to be the most promising route to a commercially viable fuel product. Ethanol production, in contrast, was modeled to require major improvements from state-of-the-art electrosynthesis to reach cost-competitiveness. Electrosynthesized formic acid from CO_2, while not initially promising as an economic fuel, was analyzed to be near market prices as a bulk chemical. Under the base case conditions reflective of state-of-the-art systems, however, none of the modeled processes were projected to be immediately on par with the commercial price of their respective liquid products. High capital costs for the CO_2 electrolyzers was a major expense in each case, necessitating high faradaic efficiency, improved current densities, and reduced electrolyzer costs per electrode area to move each process towards economic viability.

Conflicts of interest

There are no conflicts to declare.

Acknowledgements

The authors acknowledge support from the Conn Center for Renewable Energy Research at the University of Louisville.

References

1 R. S. Middleton, J. W. Carey, R. P. Currier, J. D. Hyman, Q. J. Kang, S. Karra, J. Jimenez-Martinez, M. L. Porter and H. S. Viswanathan, *Appl. Energy*, 2015, **147**, 500–509.
2 A. Otto, T. Grube, S. Schiebahn and D. Stolten, *Energy Environ. Sci.*, 2015, **8**, 3283–3297.
3 J. J. Eberhart, *Energy Efficiency and Renewable Energy*, U.S. Department of Energy – 2002 Diesel Engine Emissions Reduction (DEER) Workshop, San Diego, CA, 2002.
4 J. Qiao, Y. Liu, F. Hong and J. Zhang, *Chem. Soc. Rev.*, 2014, **43**, 631–675.
5 B. Kumar, J. P. Brian, V. Atla, S. Kumari, K. A. Bertram, R. T. White and J. Spurgeon, *Catal. Today*, 2016, **270**, 19–30.
6 B. Kumar, M. Llorente, J. Froehlich, T. Dang, A. Sathrum and C. P. Kubiak, *Annu. Rev. Phys. Chem.*, 2012, **63**(63), 541–569.
7 H.-R. M. Jhong, S. Ma and P. J. A. Kenis, *Curr. Opin. Chem. Eng.*, 2013, **2**, 191–199.
8 A. A. Peterson, F. Abild-Pedersen, F. Studt, J. Rossmeisl and J. K. Norskov, *Energy Environ. Sci.*, 2010, **3**, 1311–1315.
9 Z. W. Seh, J. Kibsgaard, C. F. Dickens, I. B. Chorkendorff, J. K. Norskov and T. F. Jaramillo, *Science*, 2017, **355**, 146.
10 T. Hatsukade, K. P. Kuhl, E. R. Cave, D. N. Abram and T. F. Jaramillo, *Phys. Chem. Chem. Phys.*, 2014, **16**, 13814–13819.
11 Y. Chen, C. W. Li and M. W. Kanan, *J. Am. Chem. Soc.*, 2012, **134**, 19969–19972.
12 C. Delacourt, P. L. Ridgway, J. B. Kerr and J. Newman, *J. Electrochem. Soc.*, 2008, **155**, B42–B49.
13 M. Asadi, B. Kumar, A. Behranginia, B. A. Rosen, A. Baskin, N. Repnin, D. Pisasale, P. Phillips, W. Zhu, R. Haasch, R. F. Klie, P. Kral, J. Abiade and A. Salehi-Khojin, *Nat. Commun.*, 2014, **5**, 4470.
14 B. A. Rosen, A. Salehi-Khojin, M. R. Thorson, W. Zhu, D. T. Whipple, P. J. A. Kenis and R. I. Masel, *Science*, 2011, **334**, 643–644.
15 A. S. Agarwal, Y. Zhai, D. Hill and N. Sridhar, *ChemSusChem*, 2011, **4**, 1301–1310.
16 T. Sekimoto, M. Deguchi, S. Yotsuhashi, Y. Yamada, T. Masui, A. Kuramata and S. Yamakoshi, *Electrochem. Commun.*, 2014, **43**, 95–97.
17 J. Wu, F. G. Risalvato, F.-S. Ke, P. J. Pellechia and X.-D. Zhou, *J. Electrochem. Soc.*, 2012, **159**, F353–F359.
18 F. Koleli and D. Balun, *Appl. Catal., A*, 2004, **274**, 237–242.
19 B. Kumar, V. Atla, J. P. Brian, S. Kumari, T. Q. Nguyen, M. Sunkara and J. M. Spurgeon, *Angew. Chem., Int. Ed.*, 2017, **56**, 3645–3649.
20 S. Zhang, P. Kang and T. J. Meyer, *J. Am. Chem. Soc.*, 2014, **136**, 1734–1737.
21 F. W. Li, L. Chen, G. P. Knowles, D. R. MacFarlane and J. Zhang, *Angew. Chem., Int. Ed.*, 2017, **56**, 505–509.
22 M. Gattrell, N. Gupta and A. Co, *J. Electroanal. Chem.*, 2006, **594**, 1–19.
23 K. P. Kuhl, E. R. Cave, D. N. Abram and T. F. Jaramillo, *Energy Environ. Sci.*, 2012, **5**, 7050–7059.
24 Y. Hori, K. Kikuchi, A. Murata and S. Suzuki, *Chem. Lett.*, 1986, 897–898.
25 Y. Hori, I. Takahashi, O. Koga and N. Hoshi, *J. Mol. Catal. A: Chem.*, 2003, **199**, 39–47.
26 S. C. Ma, M. Sadakiyo, R. Luo, M. Heima, M. Yamauchi and P. J. A. Kenis, *J. Power Sources*, 2016, **301**, 219–228.
27 T. T. H. Hoang, S. C. Ma, J. I. Gold, P. J. A. Kenis and A. A. Gewirth, *ACS Catal.*, 2017, **7**, 3313–3321.
28 X. Li, P. Anderson, H.-R. M. Jhong, M. Paster, J. F. Stubbins and P. J. A. Kenis, *Energy Fuels*, 2016, **30**, 5980–5989.
29 K. A. Keets, E. B. Cole, A. J. Morris, N. Sivasankar, K. Teamey, P. S. Lakkaraju and A. B. Bocarsly, *Indian J. Chem., Sect. A: Inorg., Bio-inorg., Phys., Theor. Anal. Chem.*, 2012, **51**, 1284–1297.
30 S. Verma, B. Kim, H.-R. M. Jhong, S. Ma and P. J. A. Kenis, *ChemSusChem*, 2016, **9**, 1972–1979.
31 M. E. Dry, *Catal. Today*, 2002, **71**, 227–241.
32 G. J. Liu, E. D. Larson, R. H. Williams, T. G. Kreutz and X. B. Guo, *Energy Fuels*, 2011, **25**, 415–437.

33 C. Graves, S. D. Ebbesen, M. Mogensen and K. S. Lackner, *Renewable Sustainable Energy Rev.*, 2011, **15**, 1–23.
34 S. D. Sajjad, Y. Gao, Z. Liu, H. Yang and R. I. Masel, *ECS Trans.*, 2017, **77**, 1653–1656.
35 D. Ren, B. S. H. Ang and B. S. Yeo, *ACS Catal.*, 2016, **6**, 8239–8247.
36 D. Ren, Y. L. Deng, A. D. Handoko, C. S. Chen, S. Malkhandi and B. S. Yeo, *ACS Catal.*, 2015, **5**, 2814–2821.
37 A. D. Handoko, C. W. Ong, Y. Huang, Z. G. Lee, L. Y. Lin, G. B. Panetti and B. S. Yeo, *J. Phys. Chem. C*, 2016, **120**, 20058–20067.
38 Y. Song, R. Peng, D. K. Hensley, P. V. Bonnesen, L. B. Liang, Z. L. Wu, H. M. Meyer, M. F. Chi, C. Ma, B. G. Sumpter and A. J. Rondinone, *ChemistrySelect*, 2016, **1**, 6055–6061.
39 C. W. Li, J. Ciston and M. W. Kanan, *Nature*, 2014, **508**, 504–507.
40 E. Bertheussen, A. Verdaguer-Casadevall, D. Ravasio, J. H. Montoya, D. B. Trimarco, C. Roy, S. Meier, J. Wendland, J. K. Norskov, I. E. L. Stephens and I. Chorkendorff, *Angew. Chem., Int. Ed.*, 2016, **55**, 1450–1454.
41 H. Yang, J. J. Kaczur, S. D. Sajjad and R. I. Masel, *ECS Trans.*, 2017, **77**, 1425–1431.
42 M. R. Shaner, H. A. Atwater, N. S. Lewis and E. W. McFarland, *Energy Environ. Sci.*, 2016, **9**, 2354–2371.
43 M. Finkenrath, *International Energy Agency*, 2011.
44 I. Dimitriou, P. Garcia-Gutierrez, R. H. Elder, R. M. Cuellar-Franca, A. Azapagic and R. W. K. Allen, *Energy Environ. Sci.*, 2015, **8**, 1775–1789.
45 G. Saur, T. Ramsden, B. James and W. Colella, *Current Central Hydrogen Production from PEM Electrolysis version 3.101, H2A Production Case Study*, US Department of Energy, 2013.
46 W. G. Colella, B. D. James and J. M. Moton, *Hydrogen Pathways Analysis for Polymer Electrolyte Membrane (PEM) Electrolysis*, Strategic Analysis, Inc., 2014.
47 B. D. James, G. N. Baum, J. Perez and K. N. Baum, *Techno-economic Analysis of Photoelectrochemical (PEC) Hydrogen Production*, US Department of Energy, 2009, pp. 71–77.
48 L.-q. Zhu, J.-l. Tu and Y.-j. Shi, *Gas Sep. Purif.*, 1991, **5**, 173–176.
49 EIA, Levelized Cost and Levelized Avoided Cost of New Generation Resources in the Annual Energy Outlook 2016, U.S. Energy Information Administration, 2016.
50 EIA, U.S. On-Highway Diesel Fuel Prices, Energy Information Administration, 2017.
51 B. Kumar, J. P. Brian, V. Atla, S. Kumari, K. A. Bertram, R. T. White and J. M. Spurgeon, *ACS Catal.*, 2016, **6**, 4739–4745.
52 A. K. Singh, S. Singh and A. Kumar, *Catal. Sci. Technol.*, 2016, **6**, 12–40.
53 D. Mellmann, P. Sponholz, H. Junge and M. Beller, *Chem. Soc. Rev.*, 2016, **45**, 3954–3988.
54 J. Eppinger and K. W. Huang, *ACS Energy Lett.*, 2017, **2**, 188–195.
55 H. S. Kheshgi and R. C. Prince, *Energy*, 2005, **30**, 1865–1871.
56 P. A. M. Claassen, J. B. van Lier, A. M. L. Contreras, E. W. J. van Niel, L. Sijtsma, A. J. M. Stams, S. S. de Vries and R. A. Weusthuis, *Appl. Microbiol. Biotechnol.*, 1999, **52**, 741–755.
57 O. Lassagne, M. C. Iliuta, L. Gosselin and M. Desilets, *Can. J. Chem. Eng.*, 2016, **94**, 761–770.
58 C. A. McMillan and G. A. Keoleian, *Environ. Sci. Technol.*, 2009, **43**, 1571–1577.
59 E. Worrell, L. Price, N. Martin, C. Hendriks and L. O. Meida, *Annu. Rev. Energy*, 2001, **26**, 303–329.